Neuromagnetic evidence for hippocampal modulation of auditory processing

茶谷, 裕

https://doi.org/10.15017/1789436

Regular Article

Neuromagnetic evidence for hippocampal modulation of auditory processing

Hiroshi Chatani[a, b], Koichi Hagiwara[a], Naruhito Hironaga[a], Katsuya Ogata[a], Hiroshi Shigeto[b], Takato Morioka[c, d], Ayumi Sakata[e], Kimiaki Hashiguchi[c], Nobuya Murakami[c], Taira Uehara[b], Jun-ichi Kira[b], and Shozo Tobimatsu[a]

Departments of Clinical Neurophysiology[a], Neurology[b] and Neurosurgery[c], Neurological Institute, Faculty of Medical Sciences, Kyushu University, Fukuoka 812-8582, Japan

[d]Department of Neurosurgery, Kyushu-Rosai Hospital, Kitakyushu 800-0296, Japan

[e]Department of Clinical Chemistry and Laboratory Medicine, Kyushu University Hospital, Fukuoka 812-8582, Japan

Correspondence should be addressed to Hiroshi Chatani, MD.
Department of Clinical Neurophysiology, Neurological Institute, Faculty of Medical Sciences, Kyushu University, 3-1-1 Maidashi, Higashi-Ku, Fukuoka 812-8582, Japan,
E-mail: chatani@neuro.med.kyushu-u.ac.jp
Telephone number: +81-92-642-5541

Abstract

The hippocampus is well known to be involved in memory, as well as in perceptual processing. To date, the electrophysiological process by which unilateral hippocampal lesions, such as hippocampal sclerosis (HS), modulate the auditory processing remains unknown. Auditory-evoked magnetic fields (AEFs) are valuable for evaluating auditory functions, because M100, a major component of AEFs, originates from auditory areas. Therefore, AEFs of mesial temporal lobe epilepsy (mTLE, n=17) with unilateral HS were compared with those of healthy (HC, n=17) and disease controls (n=9), thereby determining whether AEFs were indicative of hippocampal influences on the auditory processing. Monaural tone-burst stimuli were presented for each side, followed by analysis of M100 and a previously less characterized exogenous component (M400: 300-500 ms). The frequency of acceptable M100 dipoles was significantly decreased in the HS side. Beam-forming-based source localization analysis also showed decreased activity of the auditory area, which corresponded to the inadequately estimated dipoles. M400 was found to be related to the medial temporal structure on the HS side. Volumetric analysis was also performed, focusing on the auditory-related areas (planum temporale, Heschl's gyrus, and superior temporal gyrus), as well as the hippocampus. M100 amplitudes positively correlated with hippocampal and planum temporale volumes in the HC group, whereas they negatively correlated with Heschl's gyrus volume in the mTLE group. Interestingly, significantly enhanced M400 component was observed in the HS side of the mTLE patients. In addition, the M400 component positively correlated with Heschl's gyrus volume and tended to positively correlate with disease duration. M400 was markedly diminished after hippocampal resection. Although volumetric analysis showed decreased hippocampal volume in the HS side, the planum temporale and Heschl's gyrus, the two major sources of M100, were preserved. These results suggested that HS significantly influenced AEFs. Therefore, we concluded that the hippocampus modulates auditory processing differently under normal conditions and in HS.

Keywords

auditory-evoked magnetic fields; beam-forming analysis; hippocampal sclerosis; long-latency component; mesial temporal lobe epilepsy

1 Introduction

The hippocampus is an integral component of the medial temporal lobe memory system and recently was thought to be involved in sensory (particularly visual) perception (Graham et al., 2010; Lee et al., 2012). With respect to auditory perception, the hippocampus receives afferent inputs from the auditory association cortices, and in turn, it projects back to the primary auditory cortex and auditory association areas (Mehta et al., 2009). Within this reciprocal network, the hippocampus has been shown to inhibit redundant auditory inputs, as well as detect novel auditory information (Kraus et al., 2012). Therefore, the hippocampus is thought to play a critical role in relaying auditory information to later perceptual and cognitive processes (Parmeggiani and Rapisarda, 1969; Liberman et al., 2009; Zhang et al., 2009). However, little attention has been paid to the electrophysiological signatures of hippocampal contribution to auditory processing.

In an animal study using guinea pigs (Liberman et al., 2009), hippocampal oscillatory activity induced by auditory stimuli showed a temporal correlation with the central nucleus of the inferior colliculus, which seems to be important for later auditory processing. With regard to the relationship between the hippocampus and the auditory areas, electrical stimulation to the hippocampus enhanced or depressed responses in the auditory cortex of cats, depending on the stimulus properties (Parmeggiani and Rapisarda, 1969; Parmeggiani et al., 1982). In depth-electrode studies in humans, task-unrelated hippocampal auditory responses with peak latency at around 400 ms have been reported (Halgren et al., 1980; Grunwald et al., 2003; Boutros et al., 2008), although the precise lesion-to-response relationship was never assessed. A previous study using auditory-evoked magnetic fields (AEFs) suggested pre-attentive hippocampal influence during early stages of auditory processing at 30-120 ms (Tesche et al., 1996). The above-mentioned findings suggest that focal hippocampal lesions influence auditory-related responses. However, no clear structural-functional correlation

has been determined between the hippocampus and auditory areas both in early and late stages.

Hippocampal sclerosis (HS) is the primary pathology of mesial temporal lobe epilepsy (mTLE). With respect to auditory-related dysfunctions, mTLE patients exhibit deficits in precise detection of changes in frequency and duration of auditory stimuli, despite intact primary hearing function (Han et al., 2011). In auditory-evoked potential (AEP) studies, right HS caused left lateralized topographical changes of N100 (Rosburg et al., 2008), a major peak evoked 100 ms after the onset of auditory stimulation, and reduced N100 amplitudes were also found in mTLE (Bougeard et al., 2002). Compared with AEPs, AEFs reflect functional integrity of the auditory areas more precisely, because the neural generators of the M100 component, an MEG counterpart of the auditory N100, are located in the planum temporale and the Heschl's gyrus in each hemisphere (Näätänen et al., 1987; Ohtomo et al., 1998). Given the reciprocal connections between the hippocampus and auditory areas, it is conceivable that AEFs could reflect hippocampal contributions to the auditory processing in HS. To date, however, the process by which HS affects AEFs remains uncertain and the electrophysiological correlates have not yet been established.

Therefore, in the current study, we thoroughly examined relationships between AEFs and volumetric changes in the auditory cortices, as well as in the hippocampus. In addition, AEF components were evaluated for indications of physiological and pathophysiological alterations in the hippocampus and auditory areas.

2 Materials and methods

2.1 Subjects

Using the MEG database of adult epilepsy (2005-2014) from Kyushu University, we retrospectively identified 17 consecutive mTLE patients (eight for the right) (aged 33.8 ± 5.1 years, range: 23-58 years; 11 were female) and nine extra-temporal epilepsy patients as disease controls (DC) (six with left frontal lobe epilepsy, two with right

frontal lobe epilepsy, and one with left parietal lobe epilepsy) (aged 30.2 ± 3.1 years, range: 20-50 years; three were female). All patients fulfilled the criteria of International League Against Epilepsy (1989), and were treated with standard antiepileptic drugs (AEDs). A total of 17 volunteers (aged 33.8 ± 5.7 years, range: 21-68 years; 11 were female) were recruited as healthy controls (HC). All subjects were right-handed and had no prior history of hearing impairment or otological disorders. Inclusion criteria of mTLE were as follows: (1) MRI findings showing unilateral HS; (2) video-EEG confirmed semiology and ictal-onset localization; (3) none had extra-temporal lesions (i.e., dual pathology), prior head injury, and any other relevant histories, such as encephalitis. Eight out of the 17 consecutive mTLE patients exhibited febrile convulsions during childhood. In accordance with a previous report (Shigeto et al., 2002), inter-ictal spike foci estimated by MEG were located laterally to the hippocampus in all mTLE patients who had spikes. Thirteen mTLE patients had been treated with standard anterior temporal lobectomy, and HS was later histologically proven. Although the remaining four mTLE patients did not undergo surgical treatment, their clinical, neuroimaging, and electrophysiological characteristics were consistent with lateralized mTLE. The post-operative outcomes were evaluated using Engel's classification (Engel et al., 1993) at least 1-year post-surgery (12 out of 13 mTLE patients who underwent surgery). All mTLE patients whose outcomes were evaluated achieved optimal prognosis (six with Class Ia, five with Ib, and one with IIIa) (Table). The mTLE patients were re-grouped according to the lesion side: hemispheres with HS (HS-side group) and without HS (non-HS-side group) for statistical comparison.

With regard to DC subjects, seven out of nine DC subjects had discrete epileptic lesions which were verified by neuroimaging examinations including MRI, positron emission tomography and/or Iomazenil single photon emission CT. These lesions were concordant with the findings of ictal EEG and inter-ictal spike localization with MEG: two had focal cortical dysplasia (FCD), one contusion, one brain abscess and one encephalitis in the left frontal lobe epilepsy patients. A right frontal epilepsy patient and

a left parietal lobe epilepsy patient showed FCD. Although the remaining two DC patients were considered to have non-lesional epilepsy, their inter-ictal spikes were localized in the extra-temporal regions by MEG: one in the interhemispheric region of the right prefrontal lobe and the other in the left middle frontal gyrus. These localizations were well in accord with their semiology and ictal EEG. All DC patients were treated by the standard AEDs for localization-related epilepsy, which did not differ from those for mTLE patients. All subjects gave informed consent prior to taking part in this study. This study was approved by the Ethics Committee of Kyushu University.

2.2 Auditory stimulation

Tone-burst stimuli of 500-Hz frequency with 100-ms duration (10-ms rise and 20-ms fall) were monaurally presented with 1000-ms inter-stimulus intervals. Hearing thresholds were determined for each ear for each subject, and stimuli were delivered at intensities of 50 dB above the thresholds. Masking noises were delivered to the contralateral ear to avoid cross-hearing (Kikuchi et al., 2011). The stimuli were generated by a Tone-Burst-Generator (Kyushu-Keisokuki, Fukuoka, Japan) and were passed through plastic tubes (length, 6 m; inner diameter, 8 mm) into sponge earpieces fitted in the subjects' ears.

2.3 MRI scan

High-resolution three-dimensional MRI images were acquired using a 3-T clinical scanner (Philips Healthcare, Best, the Netherlands). Whole brain was scanned using T1-weighted fast-field echo sequence with the following parameters: repetition time = 8.2 ms; echo time = 3.8 ms; flip angle = 8 degrees; 190 sagittal slices; 1.0-mm isotropic voxels without gap. For MEG head modeling, because one mTLE patient did not undergo high-resolution imaging, we were not able to perform the localization procedures in later analyses and only confirmed the presence of HS using routine FLAIR images.

2.4 MEG recordings

AEFs were preoperatively recorded using a 306-channel whole-head system (consisting of 204 planar-type gradiometers and 102 magnetometers) (Elekta-Neuromag, Helsinki, Finland) in a quiet magnetically shielded room. Prior to the recording, four head-position-indicator coils were attached to the scalp, and a three-dimensional-digitizer (FASTRAK, Polhemus, Colchester, VT, USA) was used to measure anatomical head landmarks (bilateral pre-auricular points and nasion) and scalp surface points in reference to the head-position-indicator coils. We digitized around 200 points over the scalp surface to increase the reliability of co-registration between MEG and MRI. Head position was measured with respect to the helmet-shaped sensor array at the beginning of the recording. Magnetic responses were digitally sampled at a rate of 1000 Hz with an online band-pass filter of 0.1-330 Hz. The recordings were performed in a supine position, and the patients were instructed to stay awake but not to count or attend to the auditory stimuli. The recording was continued until at least 100 evoked responses were counted. Awareness level was also overlooked through the video monitoring system during recordings. We also applied the signal reset facility whenever external noise was observed.

2.5 Data analysis

We analyzed sensor waveforms and signal sources of M100 and M400 (a late component peaking at around 300-500 ms) in the hemispheres contralateral to the auditory stimuli. We employed a beam-forming localization method (see *2.5.4 Beam-forming analysis for M100 and M400*) to avoid any prior assumption (Van Veen et al., 1997; Huang et al., 1998; Liljeström et al., 2005) and to better localize the deeply situated activities (Ward et al., 1999). To make sure that our methodology was valid, we also applied a widely used equivalent current dipole (ECD) method to localize the M100 generator. In general, M100 can be sufficiently evaluated by equivalent current

dipole (ECD) method, because the main sources (i.e., planum temporale and Heschl's gyrus) are not deep-seated. However, the ECD analysis is not suitable to identify less dominant sources and to evaluate components with a longer duration and relatively large inter-individual variability. In addition, unlike M100, we had less prior knowledge about the M400 source, which could be deeply located in the temporal lobe, according to previous studies in which the existence of a late hippocampal component was reported (Grunwald et al., 2003; Boutros et al., 2005, 2008).

2.5.1 Preliminary process

A spatiotemporal signal space separation (tSSS) method provided by MaxFilter 2.2 software (Elekta-Neuromag) was applied as offline process to the recorded raw data to reduce artifact signals arising from outside the sensor array (Taulu et al., 2004, 2005). When artifacts due to eye movements and electrocardiogram were still present after processing with tSSS, they were carefully removed by signal-space projection function provided by minimum norm estimates (MNE) software (http://martinos.org/mne/stable/index.html) (Gramfort et al., 2014). The digitized anatomical head landmarks (bilateral pre-auricular points and nasion) and scalp surface points were co-registered onto the scalp contour extracted from the MR images. For constructing a conductor model, we created Boundary Element Method (BEM) mesh with around 600 triangular elements from the T1-weighted MRI by tessellating the inner skull surface. To compensate the head position displacement, a MaxMove command implemented in MaxFilter (Taulu et al., 2004, 2005) was applied to each sensor waveform for aligning them to the default center coordinate (0, 0, 50 mm) to relax the displacement issue so as to assess distribution of the responses in the same geometry across the runs and subjects. These MEG data were re-filtered with a band-pass filter of 0.3-58 Hz. Trials exceeding 2000 fT/cm at gradiometers and 4000 fT at magnetometers in peak-to-peak amplitude were excluded automatically from the averaging. However, at least artifact-free 100 trials were averaged using a 900-ms epoch including a 300-ms pre-stimulus period.

2.5.2 Sensor waveform analysis

Root sum square (RSS) waveforms were calculated for each pair of gradiometers. Since gradiometers show maximum amplitude just above signal sources and our primary concern was to analyze the auditory areas and mainly anterior part of the temporal lobe, we determined the sensor of interest (SOI) at the anterior to mid temporal area. We confirmed that the SOI corresponded to the distribution of group averaged RSS and used the same SOIs for all groups to minimize the selection bias (Fig. 1A). AEF amplitudes were assessed by averaging the nine sensor waveforms in the SOI with the baseline correction using -300 to -100 ms range. Here, we defined M100 as a component with the peak between 80-130 ms and M400 as a later component with its peak between 300-500 ms. For statistical comparison, averaged amplitudes were obtained for each time window. To evaluate whether HS can affect the M400 amplitude, we subtracted the amplitudes of non-HS side from those of HS side in the mTLE group, and compared them with the subtracted amplitudes of right hemisphere from left hemisphere in the HC group. Because the number of subjects in the DC group was smaller than those of other groups, the DC group results were used only for calculating the group average and a qualitative comparison with other groups. Since magnetometers are prone to low noise tolerance, we did not use magnetometers for evaluating the hemispheric difference and correlation analysis mentioned in the later section *2.5.5.* Furthermore, widely spread artificial signal centering at the vertex sensors following head position compensation (*2.5.1 preliminary process*) interfered with the sensor waveform analysis in some subjects. Therefore, we used only gradiometers for sensor waveform and correlation analyses.

2.5.3 ECD analysis for M100

ECDs were estimated using a single dipole method with realistic mono layer conductor model and BEM by SourceModeling (Elekta-Neuromag). Appropriate M100 dipoles

were determined as those fulfilling the following criteria: goodness-of-fit value > 90 %, estimated around the auditory areas (planum temporale, Heschl's gyrus, and superior temporal gyrus), and showing vertical ECD orientation towards the basal temporal region (Ohtomo et al., 1998). ECDs not fulfilling these criteria were regarded as inadequately estimated dipoles, often owing to reduced dipole strength. For each ECD iteration, the gradiometers centered at the SOI, at least 18 sensors, were selected for dipole estimation.

2.5.4 Beam-forming analysis for M100 and M400

We employed a beam-forming method to localize the M100 and M400 signal source. In principal, neuronal activity was reconstructed using a vector (linearly constrained minimum variance, LCMV) beam-forming method (Van Veen et al., 1997), which adopted the spatial filters to calculate source power for each grid distributed as the voxel space in the whole brain. We started with a definition of beam-forming output *Y* for source location *q*;

$$Y_q(\mathrm{t}) = W^T(q)m(t), \quad (1)$$

where *W* is a weight matrix for beam-forming, *m(t)* denotes the MEG measurement with time course *t* and superscript *T* denotes transpose matrix. The beam-forming weights are determined by minimizing the variance of weight signals, with subject to $W^T(q)L(q) = I$ (*L* denotes the lead field matrix, *I* denotes unit matrix). Using Lagrange multiplier, the weight matrix is given by;

$$W(q) = C^{-1}L(q)[L^T(q)C^{-1}L(q)]^{-1}, \quad (2)$$

where *C* is the covariance matrix of MEG measurement. To remove the bias of the noise, the noise normalization should be performed. The noise normalized neuronal activity index Z^2 is given by;

$$Z^2(q) = tr\{(W^T(q)CW(q)\}/tr\{W^T(q)C'W(q)\}, \quad (3)$$

where *C'* means noise covariance matrix. In addition to the basic beam-forming, some advanced algorisms are implemented in Beamformer software tool (Elekta-Neuromag).

One option is the “Event-related beamformer” which should be effective to analyze the continuous evoked data set (Robinson, 2004; Cheyne et al., 2007). The algorithm first calculates the covariance matrix C and beam-forming weight W from the whole run data. Then, signals are averaged and beam-forming power is calculated using the originally calculated weights. We employed this approach, and applied the calculation using raw data of whole 306 gradiometer and magnetometer sets with a band-pass filter of 0.3-58 Hz. The selected time window for instantaneous MEG observation (i.e. covariance matrix C) was ± 20 ms across the entire subjects for M100 generator (range; 80 ms to 120 ms) and ± 25 ms from its peak (range; 300 ms to 500 ms) for M400. For other parameter settings, we employed the default setting, including unit matrix for noise covariant matrix C' assuming that the noise was whitened, SSS transformation (i.e., SSS-beamformer (Vrba et al., 2010)) was on, regularization parameter μ for covariance matrix was 0 and so on. For head modeling and forward calculation L, realistic mono layer conductor model and BEM were employed, respectively. A source grid with 5 mm size was made for calculating the MEG lead-field matrix, which led to a grid with ~10,000 nodes covering the whole brain. This beam-forming sequentially reconstructed the activity for each voxel by selectively weighting the contribution from each MEG sensor (magnetometers and gradiometers) to a voxel's time-series.

For M100, we examined the activation power strength in the contralateral auditory area to determine whether or not it was sufficiently activated by monaural auditory stimuli in all subjects except for the DC group. Thus, when the spots on this area showed the largest or second to largest normalized power (Z^2), it was treated as sufficiently activated M100 generation. We also evaluated hippocampus contribution to M100 generation in the HC group. For M400, we carefully examined the localization in prominent cases with peak amplitudes greater than two-fold of the standard deviation and larger than the M100 peak amplitudes on the basis of the sensor waveform analysis. We also tried to show the time courses of the localized M400 source by setting virtual electrode using the Beamformer software (Elekta-Neuromag). To further clarify the

contribution of medial temporal lobe structures for M400 generation, we also recorded AEFs post-surgically in all five patients receiving regular outpatient treatment in Kyushu University Hospital.

2.5.5 Volumetric analysis and correlation analysis

Using individual MRI (section *2.3 MRI scan*), we also performed volumetric analysis of the hippocampus, planum temporale, Heschl's gyrus, and superior temporal gyrus in HC and mTLE groups using FreeSurfer software (http://surfer.nmr.mgh.harvard.edu), which has an excellent automatic volumetry tool with high correlation to visual identification (Doring et al., 2011). We overlaid the automatic delineation results on each individual MRI and confirmed if the results matched with the visually identified areas. To assess the structure-function relationship, we evaluated correlations among the AEF amplitudes and the volumetric measures (hippocampus, planum temporale, Heschl's gyrus, and superior temporal gyrus) in each group. For comparison in group average waveforms and correlation analysis, we averaged AEF amplitudes from each hemisphere in the HC group because there was no laterality between the two hemispheres (paired *t*-tests).

2.6 Statistical analysis

Statistical analyses were performed using JMP 9.0.2 (SAS Institute, Cary, NC, USA). In the sensor waveform analysis, inter-hemispheric amplitude differences were compared between mTLE patients and HC subjects using unpaired *t*-test. For the comparison of ECD strengths (dipole moment), the hemispheric differences were compared between the HS-side and HC groups using the unpaired *t*-test, and the comparison between the HS-side and non-HS-side groups was made by using the paired *t*-test. Differences in the number of inadequately estimated M100 dipoles were also statistically examined using the Pearson's chi-squared test. In the volumetric analysis, volumes and thicknesses at each cortical area were subjected to ANOVA and Tukey-Kramer's honestly significant

difference correction to test for group differences between HC, HS-side, and non-HS-side groups. The relationships between AEF amplitudes and volumetric measures were evaluated using the Pearson's correlation coefficient. Statistical significance was set at $p < 0.05$ for all analyses.

3 Results

3.1 Characteristics of M100 and M400

In RSS waveforms analysis using gradiometers, a representative left mTLE patient (Patient No.11) exhibited a less marked M100, together with a prominent auditory response emerging from 300 to 500 ms (i.e., M400) in the HS side (Fig. 1B). In contrast, M100 was preserved, but M400 was not present in the non-HS side. This trend was further confirmed by the grand average results of RSS in each group (Fig. 1C). HC group revealed a clear M100 component in the hemisphere contralateral to stimulation (Fig. 1C, upper left). However, HS-side group exhibited smaller M100 than HC and non-HS group, together with a distinct auditory response at around 400 ms (i.e., M400) (Fig. 1C, lower left). In contrast, M100 was preserved, but M400 was not present in the non-HS side group (Fig. 1C, lower right). With respect to M400, although this component seemed less prominent on the group average result because of jitter due to inter-individual variability, subtracted amplitudes of the non-HS side from HS side were significantly larger than those of HC group (Fig. 2, $p < 0.05$; unpaired t-test). There was no significant hemispheric difference for M100. In post-surgical analysis, the M400 component was diminished in all patients with prominent amplitudes prior to surgery (Fig. 3). As previously mentioned, the DC group was not quantitatively assessed. However, the group average results in the DC group were comparable to those in the HC group (Fig. 1C, upper right).

3.2 Source estimation of M100 and M400

The M100 dipoles satisfying the criteria were all estimated within the auditory area. The

inadequately estimated M100 dipoles were found mainly in the HS-side group (seven of 16 hemispheres), while they were found in only one of 17 hemispheres in the left-ear-stimulated HC group, two of 17 hemispheres in the right-ear-stimulated HC group, and two of 16 hemispheres in the non-HS-side group. Since the number of inadequately estimated M100 dipoles was significantly greater in the HS-side group than in the left-ear-stimulated HC group ($\chi^2 = 6.44$; $p < 0.05$), in the right-ear-stimulated HC group ($\chi^2 = 4.25$; $p < 0.05$), and in the non-HS-side group ($\chi^2 = 3.87$; $p < 0.05$), we could not compare ECD strengths between the groups. It is possible that lower amplitudes in some mTLE patients resulted in less acceptable dipole numbers because of low goodness-of-fit value, despite the insignificant M100 hemispheric difference in the sensor waveform analysis. In the beam-forming analysis, the incidence in which the hemisphere showed sufficient activation was least in the HS-side group (10 of 16 hemispheres). In contrast, this frequency was 100% in the left-ear-stimulated HC group, 15 of 17 hemispheres in the right-ear-stimulated HC group and 13 of 16 in the non-HS-side group. Overall, nine of 11 hemispheres showed inadequately estimated M100 dipole as well as insufficient source activation. In addition, the activation of the hippocampus was not verified by the beam-forming method in the time window of 80-120 ms. The M100 localizations in the beam-forming analysis were almost comparable with the ECD results (Fig.4A). In terms of the M400 component, their sources were medially estimated in the temporal lobe of HS side (Fig. 4B). The virtual electrode waveforms reconstructed at each M400 source showed a similar long-latency activity (i.e., M400) (Fig. 4C).

3.3 Volumetry and cortical thicknesses

ANOVA revealed a significant main effect on hippocampal volumes ($F(2,46) = 45.63$, $p < 0.0001$) and superior temporal gyrus volumes ($F(2,46) = 4.13$, $p < 0.05$). Hippocampal volumes were significantly reduced in the HS-side group compared with the HC and the non-HS-side groups ($p < 0.0001$, for both). Superior temporal gyrus

volumes were also reduced in the HS-side group compared with the HC group ($p < 0.05$) (Fig. 5), whereas volumes of the planum temporale and Heschl's gyrus showed no significant differences between the groups. In addition, there were no significant reductions in cortical thickness.

3.4 Correlation between AEFs and volumetry

M100 amplitudes positively correlated with hippocampal ($r = 0.69$, $p < 0.01$) and planum temporale volumes ($r = 0.57$, $p < 0.05$) in the HC group, while no correlation was found in the mTLE groups (HS-side and non-HS-side groups) (Fig. 6). In addition, even when these correlations were separately analyzed for both hemispheres in the HC group, M100 amplitudes and hippocampal volumes remained significantly correlated (correlation between right hippocampus and right M100 amplitude; $r = 0.53$, $p < 0.05$, correlation between left hippocampus and left M100 amplitude; $r = 0.72$, $p < 0.01$), however, no significant relationship between M100 amplitudes and planum temporale volumes was found. There was also no correlation between the M100 amplitudes and Heschl's gyrus volume in HC group, however, mTLE patients showed a significant negative correlation between M100 amplitude and the volume of Heschl's gyrus ($r = -0.54$, $p < 0.05$ in HS-side group, $r = -0.59$, $p < 0.05$ in non-HS-side group). M400 showed a significant linear correlation only with Heschl's gyrus volume ($r = 0.59$, $p < 0.05$) in HS-side group, and it tended to positively correlate with disease duration of mTLE ($r = 0.46$, $p = 0.06$) (Fig. 7).

4 Discussion

Afferent auditory input via the medial geniculate nucleus first enters the auditory areas, and is later passed on to other cortical areas and the hippocampus (Kraus et al., 2012; Mehta et al., 2009). Conversely, efferent functional connections from the hippocampus to several cortical areas, including the auditory-related areas, were shown by a depth-electrode study in humans (Catenoix et al., 2011) and by an animal study

(Cenquizca and Swanson, 2007). Electrical stimulation to the hippocampus modulated evoked responses in the cat's auditory cortex in both excitatory and inhibitory manners depending on the stimulus properties (Parmeggiani et al., 1982). In addition, a resting-state fMRI study in mTLE showed reduced functional connectivity between the auditory cortex and the hippocampus (Zhang et al., 2009). Results from a previous depth-electrode study (Catenoix et al., 2011) showed diminished evoked responses in the auditory areas in response to electrical hippocampal stimuli in patients with full-blown HS. These findings provided sufficient evidence that the hippocampus plays an important role in auditory processing. In fact, the causal relationship between auditory processing and the hippocampus has been well documented by musicogenic epilepsy, which exhibits ictal onset in the medial temporal lobe, particularly in the hippocampus, with later spread to auditory-related areas (Mehta et al., 2009). Results from the present study revealed electrophysiological signatures of hippocampal involvement in auditory processing, as well as disease-specific changes in mTLE, using the two AEF components.

4.1 M100 modulation by normal hippocampus and unilateral HS

In this study, we adopted two source localization methods (beam-forming analysis and ECD analysis) for estimating M100 generator. We found that the contralateral auditory area was mostly activated by the monaural auditory stimuli in the HC group and that the activity in the auditory area of the HS-side hemisphere was less prominent in mTLE patients. A previous study with the beam-forming technique under temporally correlated sources has pointed out that the mid-sagittal spurious sources were present in response to the binaural stimulation (Quraan and Chyene, 2010). Thus, we employed the monaural stimulation for reducing temporal correlation (Cheyne et al., 2007). The main sources of M100 are generally considered to be the planum temporale and Heschl's gyrus (Näätänen et al., 1987; Ohtomo et al., 1998; Edgar et al., 2012). From the viewpoint of correlation between AEFs and volumes, the present study revealed a

positive correlation between M100 and planum temporale volume, as well as between M100 and hippocampal volume, in the HC group. It is interesting to note that the M100 amplitudes correlated with hippocampal volume much more strongly than with planum temporale volume (see Fig. 6). Hippocampus is known to have attentional effect on various cognitive processing (Plessen et al., 2006), and N100 amplitude was significantly increased by attention (Hirata et al., 2000). A previous AEF study using the odd-ball paradigm also reported pre-attentive activity in the hippocampus in a post-stimulus time window of 30-120 ms in healthy subjects (Tesche et al., 1996). In addition, a depth-electrode study with paired-click stimuli in mTLE reported that posterior hippocampus had a response peaking at around 100 ms after the first click (Boutros et al., 2008). This indicates the possibility that the hippocampus is involved in the generation of early auditory-evoked responses. These findings suggest that N100/M100 is not merely a low order of the auditory response, and that the hippocampus has a modulatory effect on N100/M100 amplitudes ranging from pre-attentive to attentive condition. The hippocampal contribution as a modulator of M100 was not demonstrated in the beam-forming analysis of this study. Although M400 is an exogenous pathologically enhanced response, the modulatory effect for M100 may not occur as a robust evoked response. In a beam-forming analysis study (Mills et al., 2012), hippocampal activity was successfully extracted by subtracting the response in the non-memorization task from that in the memorization task, however, hippocampal activity cannot be easily separated when the subjects simply listened to the tone-burst stimuli in the task-irrelevant condition. There is also no direct evidence supporting the functional relationship between hippocampal volume and auditory processing. A previous structural MRI study demonstrated that a larger hippocampal volume results in better performance in verbal short-delay recall (Pohlack et al., 2014). Given that gray matter volume correlated with neural cell population (Pakkenberg and Gundersen, 1997), and that MEG signals corresponded with intracellular current (Kyuhou et al., 1993), it is likely that the positive correlation in the HC group could represent

hippocampal involvement during early auditory processing.

Previous AEP studies demonstrated that HS caused a topographical change of N100 (Rosburg et al., 2008) and reduction of N100 amplitudes in mTLE (Bougeard et al., 2002). In the present study, gray matter volumes were significantly decreased in the hippocampus and superior temporal gyrus but not in planum temporale gyrus in the HS-side group, suggesting that AEF changes in the HS-side group result from structural changes in these two areas. However, there was no correlation between superior temporal gyrus volume and auditory responses in the HC group and mTLE patients. A positive correlation only existed between M100 and hippocampal volume in the HC group, whereas the correlation was lost in mTLE patients, even in the non-HS side. Therefore, the pathognomonic structure-function association was only present between the hippocampus and M100 in terms of volumetric measure. Furthermore, the loss of correlation and the diminished dipole strength could represent a pathological state due to HS, because planum temporale volume remained unchanged in mTLE patients. Unilateral HS may influence activities of bilateral auditory areas, because electrical stimulation to unilateral hippocampus was shown to elicit changes of bilateral auditory cortical responses in cats (Parmeggiani et al., 1969). Unilateral hippocampal onset seizure has also been shown to spread to the contralateral hippocampus in humans (Spencer et al., 1987). These findings could explain the lack of correlation on the non-HS side.

Interestingly, in the recent results of proton magnetic resonance spectroscopy (^{1}H MRS) studies, the relationship between N-acetyl aspartate (NAA) and mTLE has attracted attention. NAA was significantly reduced in HS compared with contralateral and normal hippocampus (Hanoğlu et al., 2004). In terms of relationship between NAA and auditory response, NAA concentrations within the auditory cortex showed a significant correlation with M100 amplitudes in healthy subjects (Sörös et al., 2006). This may partly explain our results that the bigger the planum temporale volume (the larger the cell number within the region), the greater the M100 amplitudes. On the

contrary, this correlation was no longer observed in mTLE patients, despite the fact that the volume of the planum temporale was not significantly reduced. Previous studies suggested that unilateral NAA reduction in HS had remote effect on the contralateral temporal lobe as well as the ipsilateral temporal lobe (Cendes et al., 1997; Hanoğlu et al., 2004). This remote effect may underlie the loss of correlation without significant structural changes in the planum temporale both in HS side and non-HS side. Unfortunately, there is no literature that directly supports the relationship between hippocampal NAA concentration and auditory response. However, given the fact that hippocampal NAA showed a correlation with auditory verbal learning test (Hanoğlu et al., 2004), hippocampus may have some functional influences on the auditory areas. In our study, the volume of Heschl's gyrus showed a negative correlation with M100 amplitudes both in HS-side and non-HS-side group though there was no such relationship in HC group. Like the planum temporale, the volume of Heschl's gyrus was preserved in the mTLE patients. It is challenging to address these findings clearly, but at least our results support the idea that auditory processing at the stage of M100 can be modulated by an additional factor other than the structural changes of the auditory areas. In fact, similar remote structure-functional impact has also been proposed in a study with NAA in mild cognitive impairment (Li et al., 2010). Since their study showed a negative correlation between the amplitude of several auditory responses and NAA concentration in dyscognitive patients, hippocampal integrity on auditory areas may underlie the alterations in AEF responses in our study. Some authors also suggested that such abnormal relationship was attributable to the reduction of NAA in regions distant from the auditory areas with secondary modification of the auditory processing (Golob et al., 2001; Li et al., 2010).

Taken together, our results suggest that a physiological structural-functional relationship exists between normal hippocampus and auditory processing, and that HS alters the functional integrity and connection within the auditory network.

4.2 Pathognomonic significance of M400 for HS

The present study reports for the first time that M400 amplitudes were increased in the HS-side group. M400 was not detected in the HC and DC groups, but was found to be specific to HS-side and was also consistent with lateralization in the mTLE patients.

We adopted the regular tone bursts as auditory stimuli without any task demand. In previous paired-clicks studies in epileptic patients, it was reported that hippocampal auditory responses with a peak latency at around 400 ms were evoked by non-task-related stimuli of the first-click (Grunwald et al., 2003; Boutros et al., 2008) or non-target auditory stimuli in the odd-ball paradigm (Halgren et al., 1980; McCarthy et al., 1989). It was assumed that these responses reflected attention process such as novelty detection (Boutros et al., 2008) because the first-clicks were given with the long inter-pair intervals of 8-sec whereas their inter-stimulus interval was 500 ms. However, our stimuli were regularly presented with 1-sec inter-stimulus intervals, therefore, we stress that M400 can be simple auditory long-latency response related to the hippocampus and not an attention-related process as considered in previous studies. In addition, if M400 were the P300-like response, M400 amplitude should be decreased in the HS side, because reduced P300 amplitudes were reported in patients with temporal lobe epilepsy due to decreased attention (Zhang et al., 2009). However, this was not the case in the present study. Similarly, given that attention and alertness of two hemispheres were the same in each subject, larger M400 amplitudes in the HS side were hard to explain.

In addition to the exogenous as well as pathological nature of generation specifically found in mTLE, we also found marked diminution of M400 amplitude post-operatively. The M400 amplitude also showed a tendency to correlate with disease duration. A significant correlation between M400 amplitude and the Heschl's gyrus volume in the absence of volume reduction in this area indicated that auditory cortex is not the sole source of this component. On these grounds, we suggest that the hippocampus contributed to the generation of M400.

4.3 Beam-forming analysis of M400 for HS

M400 had a longer duration with relatively larger inter-individual variability. Due to the jitter caused by this variation, the component time-locked to the stimulus onset was less marked by averaging technique. Widely used distributed-source analyses such as MNE and (standardized) low resolution brain electromagnetic tomography were not suitable for M400 analysis because these techniques are generally applied to the averaged signals. It is true that these techniques can be applied also to the raw single trial, but such approach demands much time-consuming computation and inspection which made it unrealistic to apply these techniques to the current data. Hence, we adopted the beam-forming technique which does not require the averaging process. Beam-forming can be calculated based on each raw single trial with appropriate time window settings without any loss of time-locked component.

Previous epilepsy studies have not focused on M400, probably because AEPs or AEFs are typically not performed during routine evaluation for mTLE. However, beam-forming analysis revealed that M400 sources were closer to the medial temporal area when their amplitudes were prominent. The finding that the M400 source was located lateral to the hippocampus indicates two possibilities: 1) the source was situated more medially (i.e., medial temporal structures) similar to interictal spikes estimated lateral to the hippocampus by MEG, and 2) multiple sources constituted M400 and the estimated source merely reflected their center of gravity. According to a previous report, when the medial temporal lobe structure was the signal source, the estimated source tended to be lateral to the true origin (Quraan et al., 2011). Therefore, it is likely that the hippocampus works as one of the generators for M400. It was also reported that repeated electrical stimuli to the middle parahippocampal gyrus augmented evoked responses in the epileptic human hippocampus (Wilson and Engel, 1993), which was indicative of an altered excitatory-inhibitory interrelationship between the epileptogenic hippocampus and related structures. Therefore, we suggest that M400 reflected the

pathological substrate in medial temporal structures with HS, and it may exhibit a lateralizing value for mTLE.

4.4 Limitations of this study

We compared AEF responses among mTLE, HC and DC groups. Auditory responses are known to be changeable by various stimulus and physical conditions such as inter-stimulus interval, stimulus intensity, arousal and attention (see Rosburg et al., 2008). Although it seems difficult to perfectly match all conditions among all groups, we tried to keep subjects alert and did not give them any task-demand. Concerning M400, it appears that changes in conditions in each subject had little effect on our results because larger M400 in HS side was not explicable by condition difference (see *4.2 Pathognomonic significance of M400 for HS* section).

Other potential confoundedness is effect of medication. It is possible that AEDs reduce the P300 amplitude (Chayasirisobhon et al., 2007). In addition, emergence of simple auditory responses having long latency like M400 and greater P300 amplitudes have not been reported in epileptic patients taking AEDs. The fact that three out of five participants continued the same medication before and after surgery in the post-surgical analysis (patient number 2, 11 and 14, see Table) and that the response of non-HS-side group was almost the same as those of HC group suggested that M400 appearance was related to HS but not the effect of AEDs.

We found that a physiologically significant structural-functional relationship existed between normal hippocampus and auditory processing, and that HS altered the functional integrity and connection within the auditory network. To clarify these issues in detail, we need a direct proof showing how the hippocampus interacts with the supratemporal auditory cortex. The measurement of bilateral hippocampal activities, as well as activities of other related structures, with depth-electrodes while incorporating assessment of gating dysfunction may help to elucidate the contribution of the medial temporal structures to auditory processing in HS.

Since Van Veen et al. (1997) first introduced the beam-forming technique into MEG/EEG source reconstruction analysis, a number of improved beam-forming techniques with numerous applications have been proposed. In MEG research, axial gradiometers, planar gradiometers, and magnetometers are widely used. Until now, the beam-forming techniques have been mainly used in the axial type gradiometers or magnetometers. Recently, beam-forming technique has been applied to the planar type gradiometers (e.g., Vrba et. al., 2010). We have obtained successful results using both planar type gradiometers and magnetometers. However, the numbers of proposed methods, simulation studies, and neuroscientific applications for the planar type gradiometers are relatively small compared with those for the axial gradiometers. Future works on these matters should be necessary.

5 Acknowledgements

We are grateful to the statistician Associate Professor Junji Kishimoto (Department of Research and Development of Next Generation Medicine, Faculty of Medical Sciences, Kyushu University, Fukuoka, Japan) for his assistance with the statistical analysis, and to all our subjects and our colleagues for their enthusiastic cooperation. This study was supported in part by a Grant-in-Aid for Scientists, No. 24591299, from the Ministry of Education, Culture, Sports, Science and Technology in Japan. *Conflict of interest*: None declared.

References

Bougeard R, Fischer C. 2002. The role of temporal pole in auditory processing. Epileptic Disord 4:29-32.

Boutros NN, Trautner P, Rosburg T, Korzyukov O, Grunwald T, Schaller C, Elger CE, Kurthen M. 2005. Sensory gating in the human hippocampal and rhinal regions. Clin Neurophysiol 116:1967-1974.

Boutros NN, Mears R, Pflieger ME, Moxon KA, Ludowig E, Rosburg T. 2008. Sensory gating in the human hippocampal and rhinal regions: regional differences. Hippocampus 18:310-316.

Catenoix H, Magnin M, Mauguière F, Ryvlin P. 2011. Evoked potential study of hippocampal efferent projections in the human brain. Clin Neurophysiol 122:2488-2497.

Cendes F, Andermann F, Dubeau F, Matthews PM, Arnold DL. 1997. Normalization of neuronal metabolic dysfunction after surgery for temporal lobe epilepsy. Evidence from proton MR spectroscopic imaging. Neurology 49: 1525-1533.

Cenquizca LA, Swanson LW. 2007. Spatial organization of direct hippocampal field CA1 axonal projections to the rest of the cerebral cortex. Brain Res Rev 56:1-26.

Chayasirisobhon WV, Chayasirisobhon S, Tin SN, Leu N, Tehrani K, McGuckin JS. 2007. Scalp-recorded auditory P300 event-related potentials in new-onset untreated temporal lobe epilepsy. Clin EEG Neurosci 38:168-171.

Cheyne D, Bostan AC, Gaetz W, Pang EW. 2007. Event-related beamforming: a robust method for presurgical functional mapping using MEG. Clin Neurophysiol 118: 1691-1704.

Commission on Classification and Terminology of the International League Against Epilepsy. 1989. Proposal for revised classification of epilepsies and epileptic syndromes. Epilepsia 30:389-399.

Doring TM, Kubo TT, Cruz LC Jr, Juruena MF, Fainberg J, Domingues RC, Gasparetto EL. 2011. Evaluation of hippocampal volume based on MR imaging in patients with bipolar affective disorder applying manual and automatic segmentation techniques. J Magn Reson Imaging 33:565-572.

Edgar JC, Hunter MA, Huang M, Smith AK, Chen Y, Sadek J, Lu BY, Miller GA, Cañive JM. 2012. Temporal and frontal cortical thickness associations with M100 auditory activity and attention in healthy controls and individuals with schizophrenia. Schizophr Res 140:250-257.

Engel Jr J, Van Ness PC, Rasmussen TB, Ojemann LM. 1993. Outcome with respect to epileptic seizures. In: Engel Jr J, editor. Surgical treatment of the epilepsies. 2nd ed. New York: Raven Press. pp 609-621.

Golob EJ, Johnson JK, Starr A. 2002. Auditory event-related potentials during target detection are abnormal in mild cognitive impairment. Clin Neurophysiol 113:151-161.

Graham KS, Barense MD, Lee ACH. 2010. Going beyond LTM in the MTL: a synthesis of neuropsychological and neuroimaging findings on the role of the medial temporal lobe in memory and perception. Neuropsychologia 48:831-853.

Gramfort A, Luessi M, Larson E, Engemann DA, Strohmeier D, Brodbeck C, Parkkonen L, Hämäläinen MS. 2014. MNE software for processing MEG and EEG data. Neuroimage 86:446-460.

Grunwald T, Boutros NN, Pezer N, von Oertzen J, Fernández G, Schaller C, Elger CE. 2003. Neuronal substrates of sensory gating within the human brain. Biol Psychiatry 53:511-519.

Halgren E, Squires NK, Wilson CL, Rohrbaugh JW, Babb TL, Crandall PH. 1980. Endogenous potentials generated in the human hippocampal formation and amygdala by infrequent events. Science 210:803-805.

Han MW, Ahn JH, Kang JK, Lee EM, Lee JH, Bae JH, Chung JW. 2011. Central auditory processing impairment in patients with temporal lobe epilepsy. Epilepsy Behav 20:370-374.

Hanoğlu L, Ozkara C, Keskinkiliç C, Altin U, Uzan M, Tuzgen S, Dinçer A, Ozyurt E. 2004. Correlation between 1H MRS and memory before and after surgery in mesial temporal lobe epilepsy with hippocampal sclerosis. Epilepsia 45: 632-640.

Hirata K, Hozumi A, Tanaka H, Kubo J, Zeng XH, Yamazaki K, Asahi K, Nakano T. 2000. Abnormal information processing in dementia of Alzheimer type. A study using the event-related potential's field. Eur Arch Psychiatry Clin Neurosci 250: 152-155.

Huang M, Aine CJ, Supek S, Best E, Ranken D, Flynn ER. 1998. Multi-start downhill simplex method for spatio-temporal source localization in magnetoencephalography. Electroencephalogr Clin Neurophysiol 108:32-44.

Kikuchi Y, Ogata K, Umesaki T, Yoshiura T, Kenjo M, Hirano Y, Okamoto T, Komune S, Tobimatsu S. 2011. Spatiotemporal signatures of an abnormal auditory system in stuttering. Neuroimage 55:891-899.

Kraus KS, Canlon B. 2012. Neuronal connectivity and interactions between the auditory and limbic systems: effects of noise and tinnitus. Hear Res 288:34-46.

Kyuhou S, Okada YC. 1993. Detection of magnetic evoked fields associated with synchronous population activities in the transverse CA1 slice of the guinea pig. J Neurophysiol 70:2665-2668.

Lee ACH, Yeung LK, Barense MD. 2012. The hippocampus and visual perception. Front Hum Neurosci 6:91.

Li X, Shao X, Wang N, Wang T, Chen G, Zhou H. 2010. Correlation of auditory event-related potentials and magnetic resonance spectroscopy measures in mild cognitive impairment. Brain Res 30: 204-212.

Liberman T, Velluti RA, Pedemonte M. 2009. Temporal correlation between auditory neurons and the hippocampal theta rhythm induced by novel stimulations in awake guinea pigs. Brain Res 17:70-77

Liljeström M, Kujala J, Jensen O, Salmelin R. 2005. Neuromagnetic localization of rhythmic activity in the human brain: a comparison of three methods. Neuroimage 25:734-745.

McCarthy G, Wood CC, Williamson PD, Spencer DD. 1989. Task-dependent field potentials in human hippocampal formation. J Neurosci 9:4253-4268.

Mehta AD, Ettinger AB, Perrine K, Dhawan V, Patil A, Jain SK, Klein G, Schneider SJ, Eidelberg D. 2009. Seizure propagation in a patient with musicogenic epilepsy. Epilepsy Behav 14:421-424.

Mills T, Lalancette M, Moses SN, Taylor MJ, Quraan MA. 2012. Techniques for detection and localization of weak hippocampal and medial frontal sources using beamformers in MEG. Brain Topogr 25: 248-263.

Näätänen R, Picton T. 1987. The N1 wave of the human electric and magnetic response to sound: a review and an analysis of the component structure. Psychophysiology 24:375-425.

Ohtomo S, Nakasato N, Kanno A, Hatanaka K, Shirane R, Mizoi K, Yoshimoto T. 1998. Hemispheric asymmetry of the auditory evoked N100m response in relation to the crossing point between the central sulcus and Sylvian fissure. Electroencephalogr Clin Neurophysiol 108:219-225.

Pakkenberg B, Gundersen HJ. 1997. Neocortical neuron number in humans: effect of sex and age. J Comp Neurol 384:312-320.

134 Parmeggiani PL, Rapisarda C. 1969. Hippocampal output and sensory mechanisms.
135 Brain Res 14:387-400.
136
137 Parmeggiani PL, Lenzi P, Azzaroni A, D'Alessandro R. 1982. Hippocampal influence on
138 unit responses elicited in the cat's auditory cortex by acoustic stimulation. Exp Neurol
139 78:259-274.
140
141 Plessen KJ, Bansal R, Zhu H, Whiteman R, Amat J, Quackenbush GA, Martin L,
142 Durkin K, Blair C, Royal J, et al. 2006. Hippocampus and amygdala morphology in
143 attention-deficit/hyperactivity disorder. Arch gen Psychiatry 63: 795-807.
144
145 Pohlack ST, Meyer P, Cacciaglia R, Liebscher C, Ridder S, Flor H. 2014. Bigger is
146 better! Hippocampal volume and declarative memory performance in healthy young
147 men. Brain Struct Funct 219:255-267.
148
149 Quraan MA, Cheyne D. 2010. Reconstruction of correlated brain activity with adaptive
150 spatial filters in MEG. Neuroimage 49:2387-2400.
151
152 Quraan MA, Moses SN, Hung Y, Mills T, Taylor MJ. 2011. Detection and localization
153 of hippocampal activity using beamformers with MEG: a detailed investigation using
154 simulations and empirical data. Hum Brain Mapp 32:812-827.
155
156 Robinson SE. 2004. Localization of event-related activity by SAM(erf). Neurol Clin
157 Neurophysiol 30: 73.
158
159 Rosburg T, Boutros NN, Ford JM. 2008. Reduced auditory evoked potential component
160 N100 in schizophrenia--a critical review. Psychiatry Res 161:259-274.

Rosburg T, Trautner P, Ludowig E, Helmstaedter C, Bien CG, Elger CE Boutros NN. 2008. Sensory gating in epilepsy: effects of the lateralization of hippocampal sclerosis. Clin Neurophysiol 119:1310-1319.

Shigeto H, Morioka T, Hisada K, Nishio S, Ishibashi H, Kira D, Tobimatsu S, Kato M. 2002. Feasibility and limitations of magnetoencephalographic detection of epileptic discharges: simultaneous recording of magnetic fields and electrocorticography. Neurol Res 24:531-536.

Sörös P, Michael N, Tollkötter M, Pfleiderer B. 2006. The neurochemical basis of human cortical auditory processing: combining proton magnetic resonance spectroscopy and magnetoencephalography. BMC Biol 4: 25.

Spencer SS, Williamson PD, Spencer DD, Mattson RH. 1987. Human hippocampal seizure spread studied by depth and subdural recording: the hippocampal commissure. Epilepsia 28:479-489.

Taulu S, Simola J, Kajola M. 2004. MEG recordings of DC fields using the signal space separation method (SSS). Neurol Clin Neurophysiol 35:1-4.

Taulu S, Simola J, Kajola M. 2005. Applications of the signal space separation method. IEEE Trans Signal Process 53:3359-3372.

Tesche CD, Karhu J, Tissari SO. 1996. Non-invasive detection of neuronal population activity in human hippocampus. Brain Res Cogn Brain Res 4:39-47.

188 Van Veen BD, van Drongelen W, Yuchtman M, Suzuki A. 1997. Localization of brain
189 electrical activity via linearly constrained minimum variance spatial filtering. IEEE
190 Trans Biomed Eng 44:867-880.
191
192 Vrba J, Taulu S, Nenonen J, Ahonen A. 2010. Signal space separation beamformer.
193 Brain Topogr 23: 128-133.
194
195 Ward DM, Jones RD, Bones PJ, Carroll GJ. 1999. Enhancement of deep epileptiform
196 activity in the EEG via 3-D adaptive spatial filtering. IEEE Trans Biomed Eng
197 46:707-716.
198
199 Wilson CL, Engel J Jr. 1993. Electrical stimulation of the human epileptic limbic cortex.
200 Adv Neurol 63:103-113.
201
202 Zhang Z, Lu G, Zhong Y, Tan Q, Liao W, Chen Z, Shi J, Liu Y. 2009. Impaired
203 perceptual networks in temporal lobe epilepsy revealed by resting fMRI. J Neurol
204 256:1705-1713.
205
206 Zhang Z, Lu G, Zhong Y, Tan Q, Yang Z, Liao W, Chen Z, Shi J, Liu Y. 2009. Impaired
207 attention network in temporal lobe epilepsy: a resting FMRI study. Neurosci Lett
208 453:97-101.

Figure legends

Figure 1. Group average RSS of AEFs (gradiometers) to the left ear stimulation in HC subjects (A). The nine sensor sets contralateral to the stimulation (solid-line ellipse) and sensor sets on the ipsilateral side (dashed-line ellipse) are highlighted. The former is defined as the SOIs for the averaged RSS. A dashed-line square indicates an ill-defined M100 in a representative left mTLE patient (Patient No.11) in the HS side in response to right ear stimulation (B). Note that, as indicated by the ellipses, a prominent response with its peak at around 300-500 ms (i.e., M400) is observed in the HS side, while M400 is absent with preserved M100 (inverted triangles) in the non-HS side. Group average results of RSS (gradiometer) in each group (C). M100 was identified in all groups (inverted triangles), while only the HS-side group exhibited a distinct response with its peak at around 300-500 ms (M400) (solid and thick-line ellipse). M100 amplitude seemed to be slightly reduced in the HS-side group compared with HC group and non-HS-side group, but no statistical significance was found (see *3.1 Characteristics of M100 and M400*). Note that the RSS amplitudes exceed below zero at some time points, which resulted from the baseline correction (see *2.5.2 Sensor waveform analysis*) in this and subsequent figures.

Figure 2. Scatter plots of M100 and M400 amplitudes (hemispheric difference) for comparison between the HC and mTLE subjects. Firstly, subtracted amplitudes of the non-HS side from HS side were calculated in each mTLE patient. Secondly, subtracted amplitudes of right hemisphere from left hemisphere were calculated in each HC subject. Thirdly, unpaired *t*-test was used to compare hemispheric difference between HC subjects and mTLE patients. There was no significant hemispheric difference in the M100 amplitude (averaged across the 80- to 130-ms time window) (Left). Subtracted M400 amplitudes (averaged across the 300- to 500-ms time window) of the non-HS side

from HS side were significantly larger than those of HC group ($p < 0.05$; unpaired *t*-test) (Right). Error bars represent standard errors.

Figure 3. Effect of surgical resection of hippocampus on the M400 component. The post-stimulus period of 300-500 ms in squares shows M400 components (a solid square; pre-surgery, a dashed-line square; post-surgery). Pt. No. 5 and 14 revealed no interval change as a result of no clear M400 in the pre-surgical condition. All other patients (Pts. No. 2, 11, and 12) exhibited a clear reduction in amplitude post-surgery.

Figure 4. Source localization of M100 and M400. (A) A representative M100 source in a healthy control evoked by left auditory stimulation. Left figure shows the result of ECD analysis while right figure illustrates the result of beam-forming analysis (80-120 ms). (B) M400 sources of the mTLE patients with prominent M400 estimated by beam-forming method (see *2.5.4 Beam-forming analysis for M100 and M400*). (C) Time courses at the M400 sources estimated in the virtual electrodes. Each subject showed M400 peaking at around 300-500 ms (M400, red ellipse).

Figure 5. Volumetric analysis of the hippocampus and auditory-related areas (superior temporal gyrus, Heschl's gyrus and planum temporale). Volumes of hippocampus and superior temporal gyrus were significantly reduced in the HS-side group (hippocampus ($F(2,46) = 45.63$, $p < 0.0001$), superior temporal gyrus ($F(2,46) = 4.13$, $p < 0.05$). In contrast, Heschl's gyrus and the planum temporale showed no volume reductions. Error bars represent standard errors.

Figure 6. Correlation analysis between M100 amplitudes and volumes of temporal structures in the HC, HS-side, and non-HS-side groups. The scatterplots show the relationship between M100 amplitude and anatomical volumes. In the HC group, the

263 M100 amplitude revealed a strong linear positive correlation with hippocampal volume
264 ($r = 0.69$, $p < 0.01$) and also a modest linear positive correlation with planum temporale
265 volume ($r = 0.57$, $p < 0.05$). In the HS-side and non-HS-side groups, the M100
266 amplitude showed a negative correlation with Heschl's gyrus volume ($r = -0.54$, $p <$
267 0.05 in HS-side group, $r = -0.59$, $p < 0.05$ in non-HS-side group), while HC group no
268 correlation with this area.
269
270 **Figure 7.** Correlation analysis between M400 amplitudes and Heschl's gyrus volume
271 (HS-side group) and disease duration. The M400 amplitude showed a positive
272 correlation with Heschl's gyrus volume ($r = 0.59$, $p < 0.05$). Disease duration showed a
273 trend to positively correlate with the M400 amplitudes ($r = 0.46$, $p = 0.06$).

Table. Clinical features of mTLE patients.

Patients	Clinical diagnosis	Sex	Age (years)	Onset (years)	EEG (interictal)	EEG (ictal)	MEG	Surgical outcome
1	Rt mTLE	F	25	12	Rt-aT	Rt-T	Rt-T	Ia
2	Rt mTLE	M	25	7	Bil-T	Rt-T	Rt-T	Ia
3	Rt mTLE	F	28	14	Rt-T+F	Rt-T+F	Rt-T	Ia
4	Rt mTLE	M	39	3	Rt-T	Rt-T	Rt-T	Ib
5	Rt mTLE	F	33	11	Rt	Rt-T+F	No spike	Ib
6	Rt mTLE	M	23	14	Bil-T	Rt-T	Bil-T	Ib
7	Rt mTLE	M	24	7	Rt-aT	NA	Rt-T	NA
8	Rt mTLE	F	28	16	Rt-aT	Rt-T	Rt-T	NA
9	Lt mTLE	F	31	12	Lt-T	Lt-aT	Lt-T	Ib
10	Lt mTLE	F	34	12	Lt-aT	Lt-aT	Lt-T	Ia
11	Lt mTLE	F	58	10	Bil-T	Lt-T	Lt-T	IIIa
12	Lt mTLE	F	39	7	Lt-aT	Lt-T	Lt-T	Ib
13	Lt mTLE	M	52	12	Lt-aT	Lt-aT	Lt-T	NA
14	Lt mTLE	F	33	2	Lt-aT	Lt-aT	No spike	Ia
15	Lt mTLE	F	32	3	No spike	Lt-aT	No spike	Ia
16	Lt mTLE	M	46	31	Bil-T	Lt-hippocampus*	Bil-T	NA
17	Lt mTLE	F	25	24	Lt-T	NA	Lt-T	NA

Surgical outcome was classified according to Engel's classification (1993). In patient 16, ictal onset was determined by depth-electrode recording (indicated by an asterisk). aT = anterior temporal; T = temporal; F = frontal; NA = not applicable.

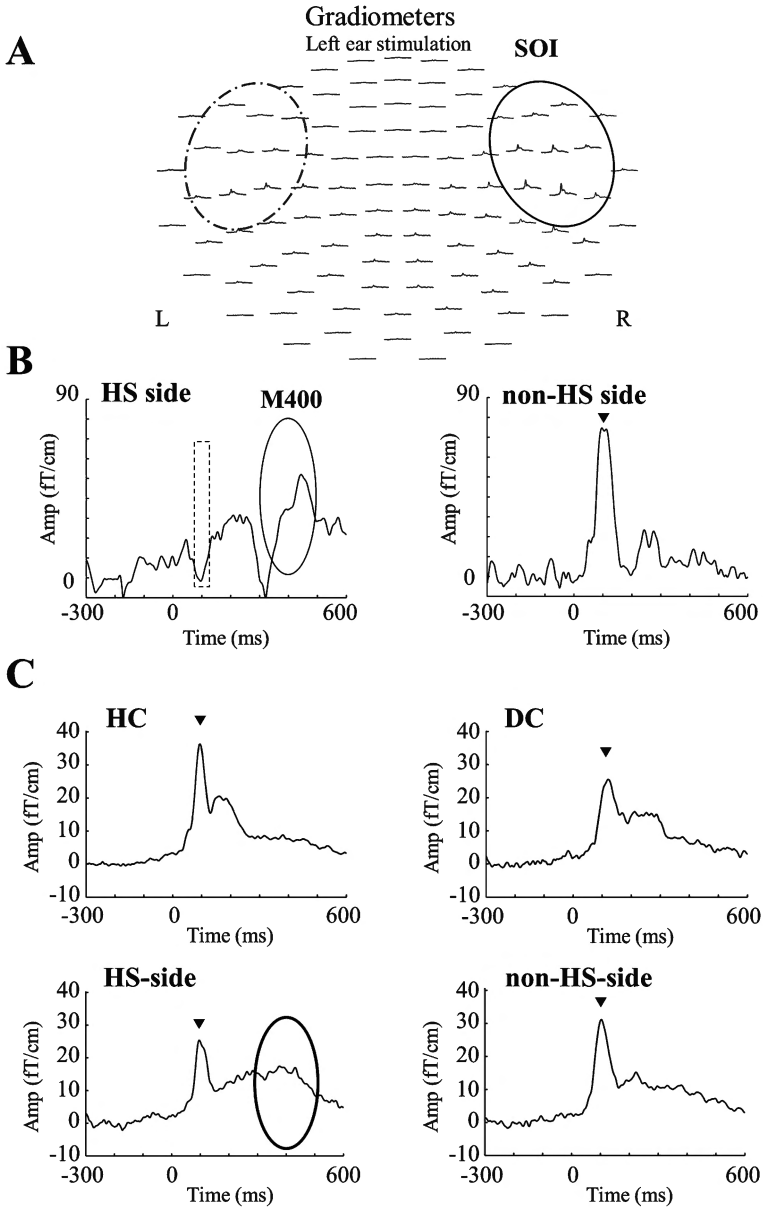
A
Gradiometers
Left ear stimulation
SOI
L
R
B
HS side
M400
non-HS side
90
0
Amp (fT/cm)
-300
0
600
Time (ms)
C
HC
DC
HS-side
non-HS-side
40
30
20
10
0
-10

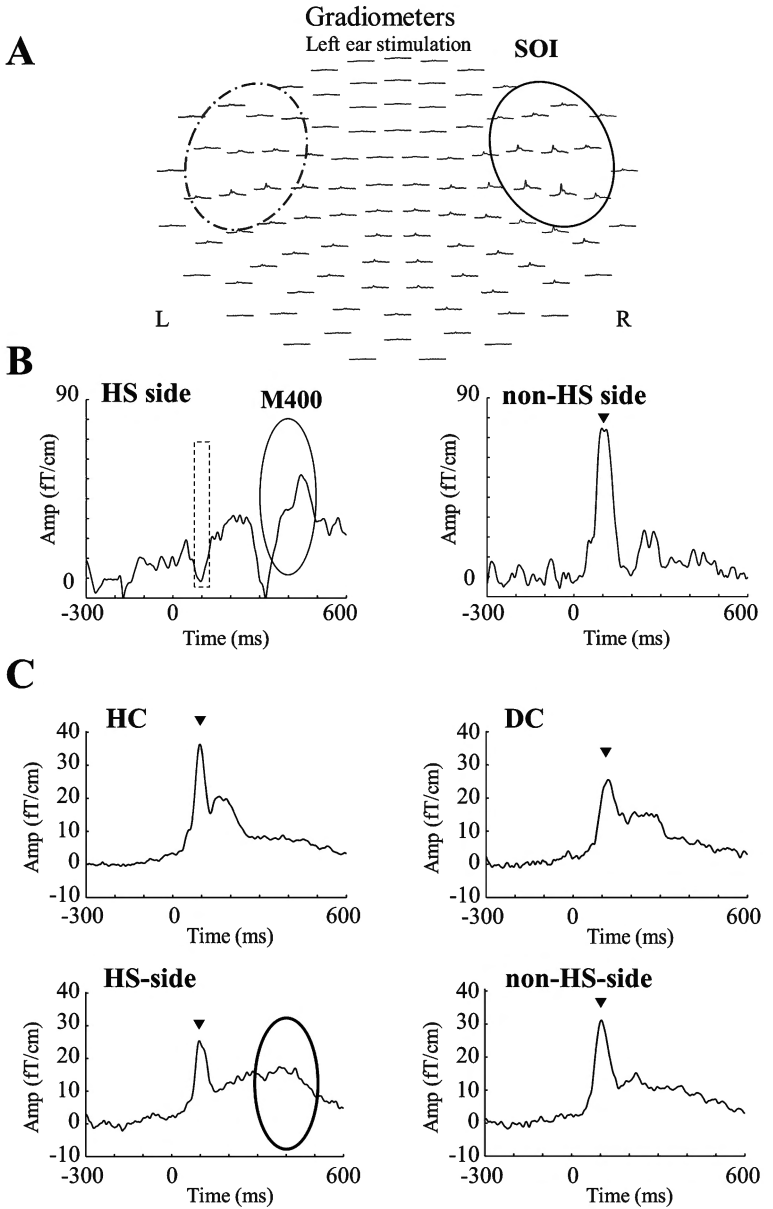
A
Gradiometers
Left ear stimulation
SOI
L
R
B
HS side
M400
non-HS side
90
0
Amp (fT/cm)
-300
0
600
Time (ms)
C
HC
DC
HS-side
non-HS-side
40
30
20
10
0
-10

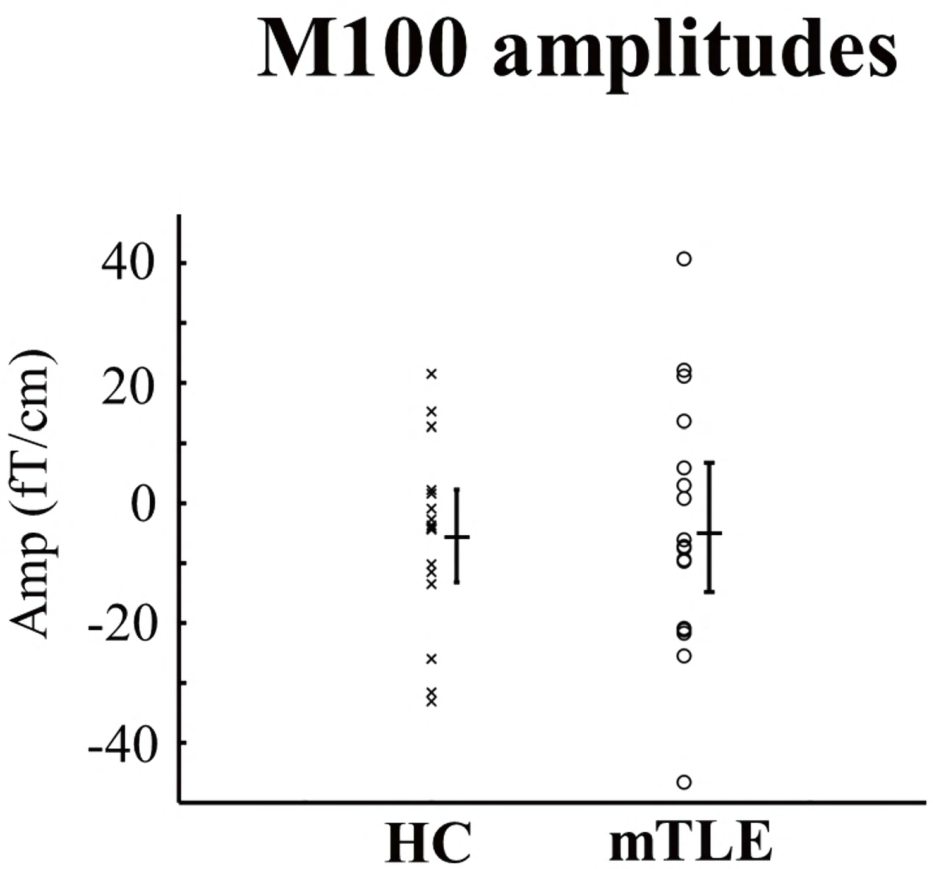
M100 amplitudes
Amp (fT/cm)
40
20
0
-20
-40
HC
mTLE

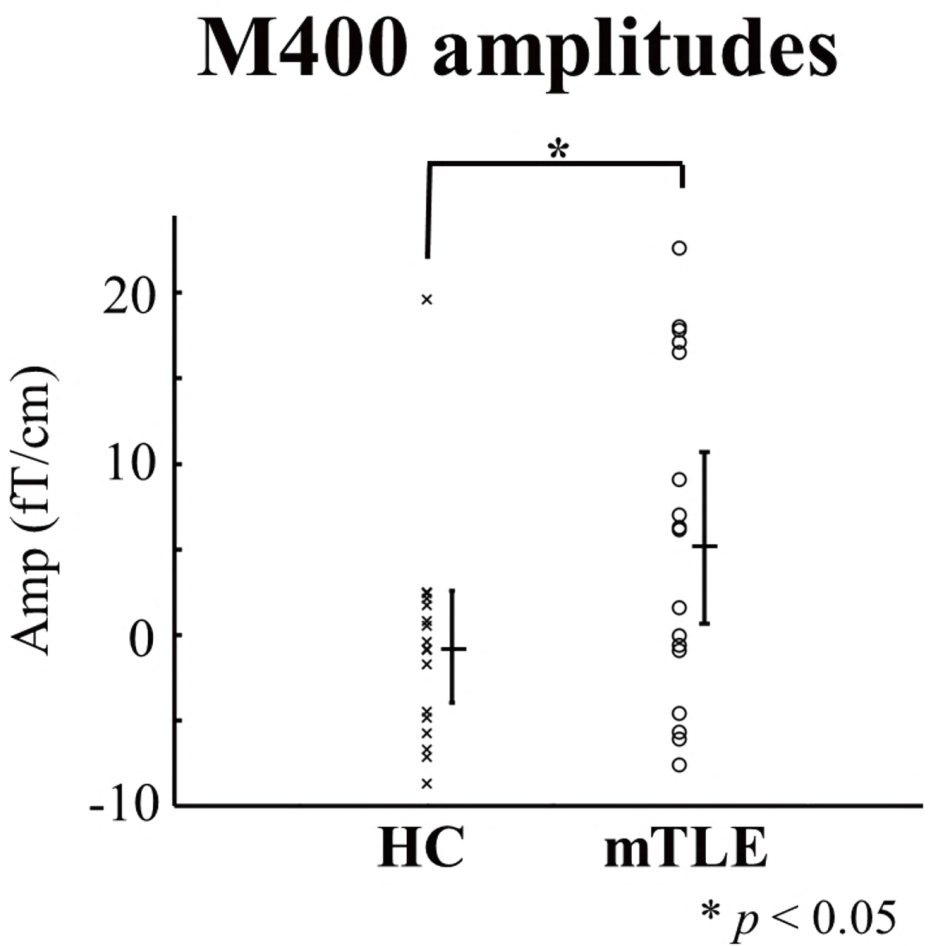
M400 amplitudes
*
Amp (fT/cm)
20
10
0
-10
HC
mTLE
* $p < 0.05$

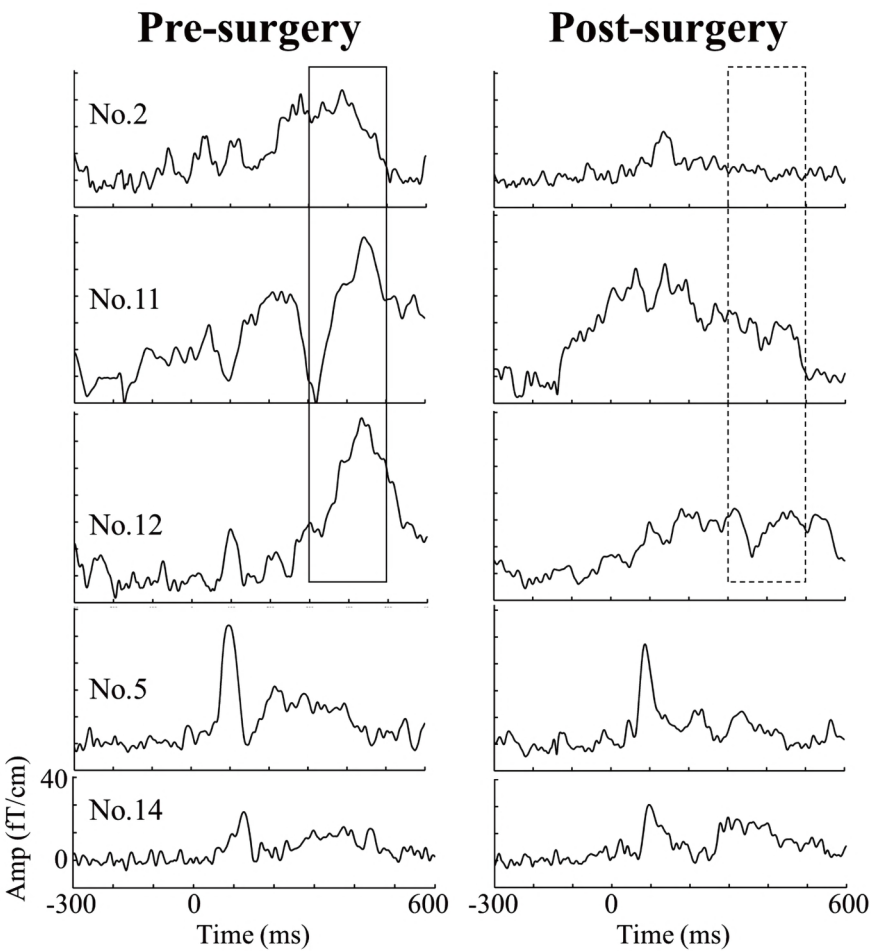
Pre-surgery
Post-surgery
No.2
No.11
No.12
No.5
No.14
40
0
Amp (fT/cm)
-300
0
600
Time (ms)
-300
0
600
Time (ms)

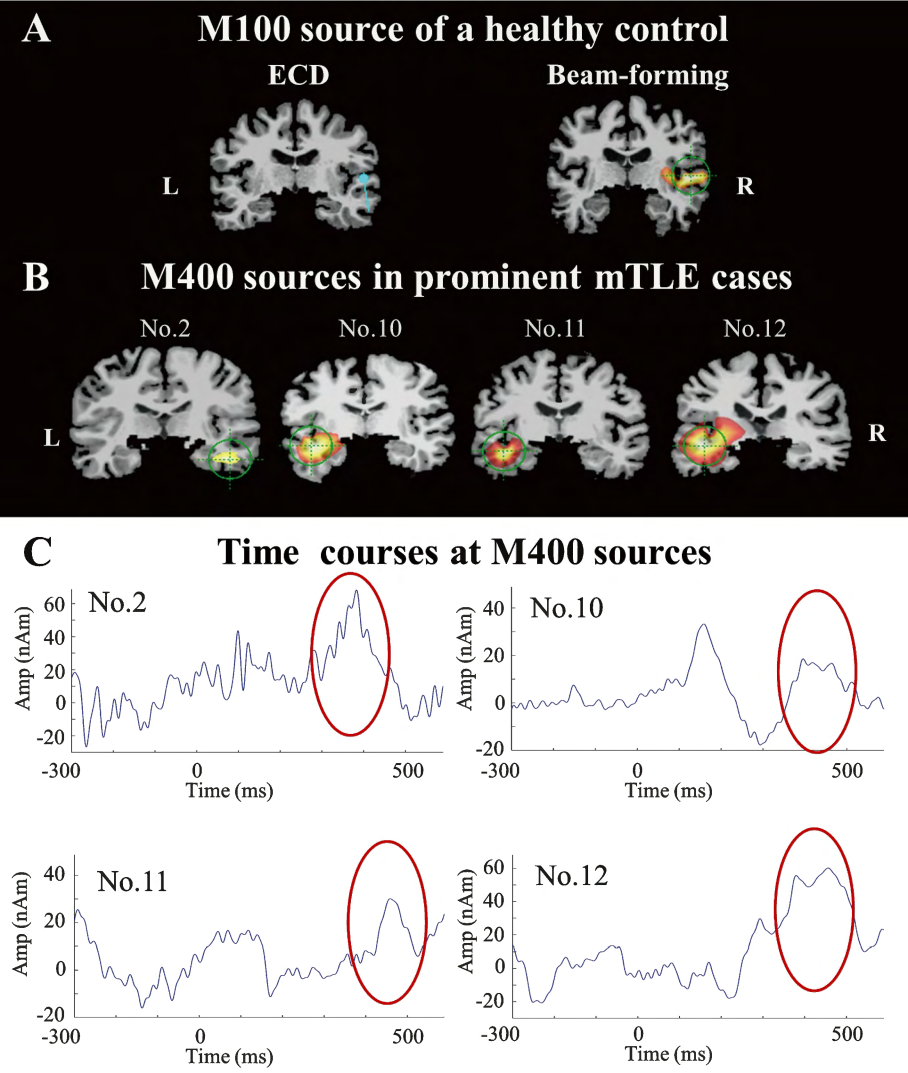
A
M100 source of a healthy control
ECD
Beam-forming
L
R
B
M400 sources in prominent mTLE cases
No.2
No.10
No.11
No.12
L
R
C
Time courses at M400 sources
No.2
No.10
No.11
No.12
Amp (nAm)
Time (ms)
-300
0
500
60
40
20
0
-20

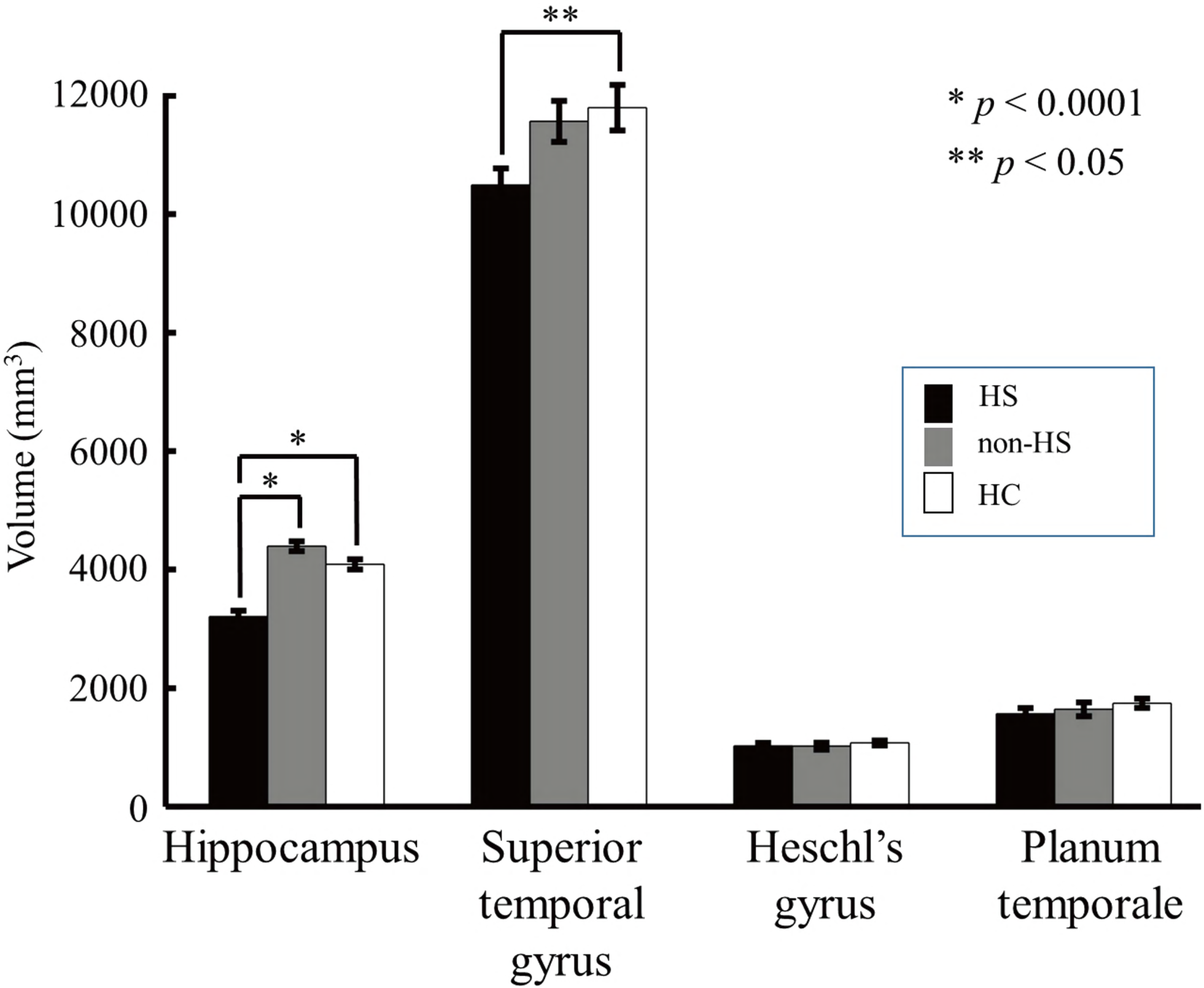
12000
10000
8000
6000
4000
2000
0
Volume (mm3)
**
*
*
* p < 0.0001
** p < 0.05
HS
non-HS
HC
Hippocampus
Superior temporal gyrus
Heschl's gyrus
Planum temporale

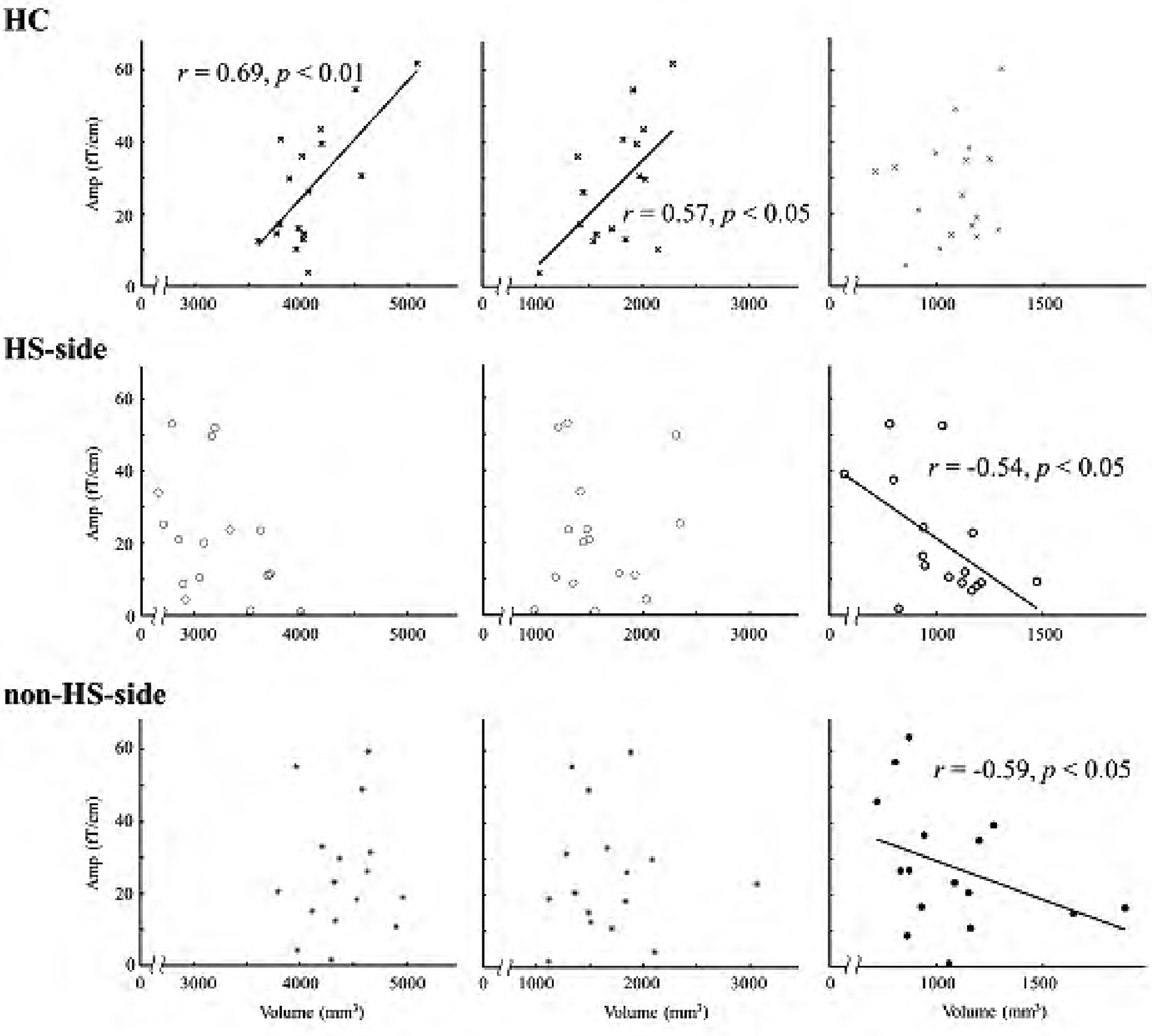
HC
HS-side
non-HS-side
r = 0.69, p < 0.01
r = 0.57, p < 0.05
r = -0.54, p < 0.05
r = -0.59, p < 0.05
Amp (fT/cm)
Volume (mm³)
Hippocampus
Planum temporale
Heschl's gyrus

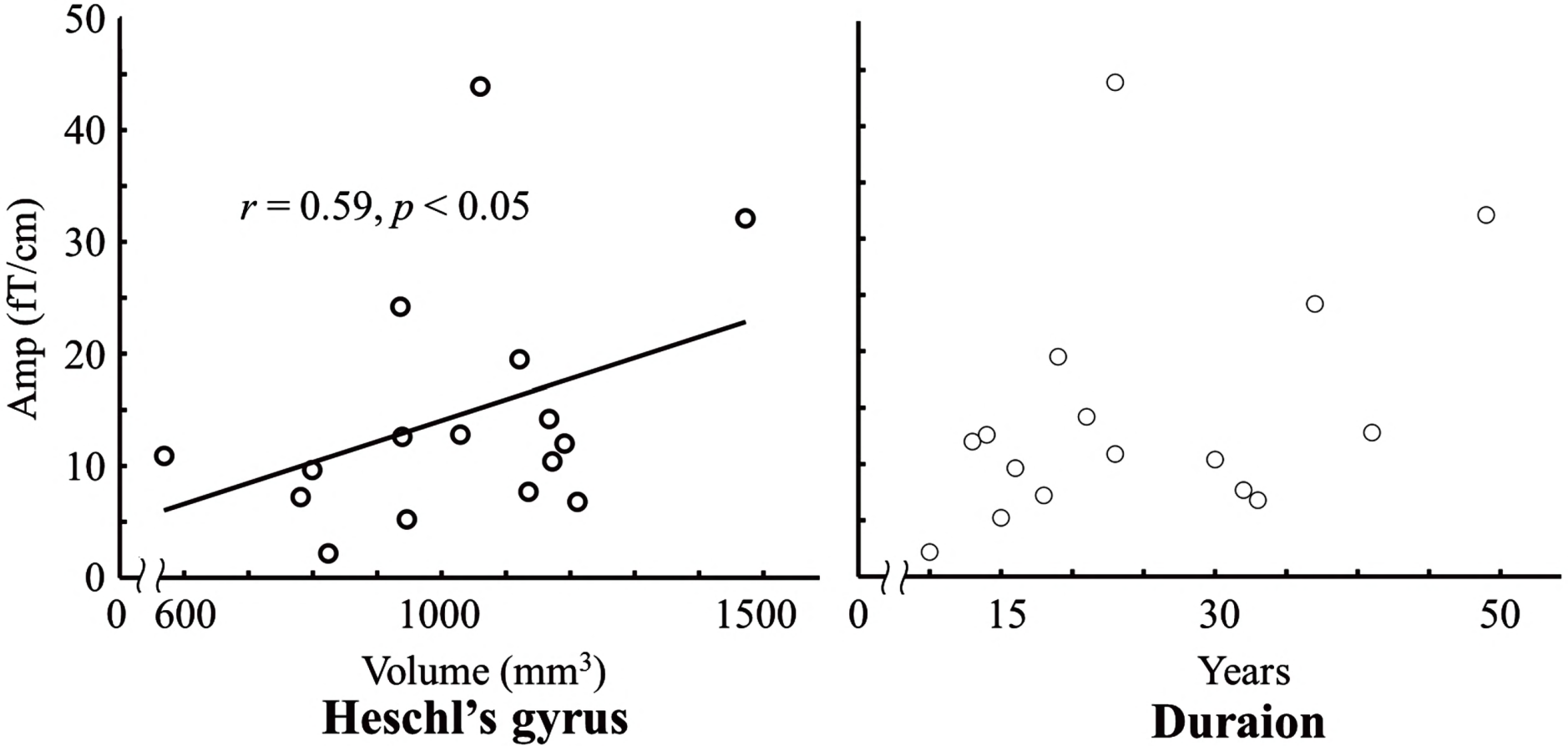
50
40
30
20
10
0
Amp (fT/cm)
$r = 0.59, p < 0.05$
0
600
1000
1500
Volume (mm³)
Heschl's gyrus
0
15
30
50
Years
Duraion